Supporting Information

Precisely Modulating of Chromatin Tracker *via* Substituent Engineering: Reporting Pathological Oxidative Stress during Mitosis

Jinsong Li,[1 a] Yingyong Ni,[1 a] Junjun Wang,*[a] Yicai Zhu, [a] Aidong Wang, [c] Xiaojiao Zhu, [a] Xianshun Sun, [a] Sen Wang, [a] Dandan Li, [a] Hongping Zhou*[a, b]

[a] *School of Chemistry and Chemical Engineering, School of Materials Science and Engineering, Institute of Physical Science and Information Technology, Center of Free Electron Laser & High Magnetic Field, Key Laboratory of Structure and Functional Regulation of Hybrid Materials Ministry of Education, Key Laboratory of Functional Inorganic Materials Chemistry of Anhui Province, and Key Laboratory of Chemistry for Inorganic/Organic Hybrid Functionalized Materials of Anhui Province, Anhui University, Hefei, 230601, P.R. China*

[b] *School of Chemical and Environmental Engineering, Anhui Polytechnic University, Wuhu, 241000, P.R. China.*

[c] *Key Laboratory of drug design, Huangshan University, Huangshan, 245021, P.R. China*

1. Experimental Procedures

1.1 Chemicals and Materials

Chemicals and solvents were used as received without further purification. The chemical reagents including 2-methylbenzothiazole, 3-bromopropyne, 3-bromopropionic acid, 4-(diethylamino)salicylaldehyde, diethyl malonate, piperidine and so on were purchased from Aladdin or Macklin *Co., Ltd*. The other solvents and reagents in experiments were analytically pure grade. 2,7-Dichlorodihydrofluorescein diacetate (DCFH-DA), singlet oxygen sensor green (SOSG), 9, 10-anthracenedipropanoicacid (ABDA), 5,5-dimethyl-1-pyrroline N-oxide (DMPO), rose bengal (RB), *γ*-H2AX immunostaining kit, BODIPY493/503, 4',6-diamidino-2-phenylindole (DAPI), 3- (4, 5-dimethylthiazol-2-yl)-2, 5-diphenyltetrazolium bromide (MTT) and so on, were obtained from the reagent company (Sigma-Aldrich, Bioquest, Thermo *Co., Ltd*). The HepG2 (human hepatocellular carcinoma cells), HeLa (human cervical cancer cells), A293T (human renal epithelial cells), and HUVEC (human umbilical vein endothelial cells) cells were acquired from BeNa culture collection.

1.2 Instrumentation

^{1}H-NMR and ^{13}C-NMR spectra of **CBTZ-yne**, **CBTZ-acid** and intermediate products were tested on Bruker AVANCE-400 MHz and 100 MHz NMR instruments with solvent of DMSO-d_6 or Methanol-d_4, respectively. Mass spectrometric (MS) data were obtained by Thermo Fisher Scientific LTQ-Orbitrap XL mass spectrometer using a positive electrospray ionization (ESI^+). Absorption and emission spectra for **CBTZ-yne** and **CBTZ-acid** were measured on UV-265 spectrophotometer and Hitachi F-4500 fluorescence spectrophotometer, respectively. The electron paramagnetic resonance (EPR) spectra were recorded by the Nano X-band system from Bruker (Germany). Cell imaging was recorded on a confocal laser scanning microscope (Laica TCS SP8 DIVE/SP8 DIVE) with 60×objective lens, and the pictures were processed by ImageJ software.

1.3 Synthetic and Characterization

The 2-methyl-3-(prop-2-yn-1-yl)benzo[d]thiazol-3-ium, bromide (**1**), 7-diethylamino-3-formylcoumarin (**2**), 3-(2-carboxyethyl)-2-methylbenzo[d]thiazol-3-ium, bromide (**3**) were prepared according to the literatures.[1-3]

CBTZ-yne: Compounds **1** and **2** were reacted by Knoevenagel to obtain the target product **CBTZ-yne**. **1** (0.80 g, 0.003 mol) and **2** (0.74 g, 0.003 mol) were refluxed with 0.2 mL of piperidine in 15.0 mL methanol for 4 h. After the reaction was complete, the solvent was evaporated. Then, the crude product was purified by silica gel column chromatography (CH_2Cl_2: CH_3OH = 10: 1, v/v) to get **CBTZ-yne** as the dark purple powdered solid (0.59 g, 40%). ^{1}H NMR (400 MHz, DMSO-d_6), δ (ppm) (Figure S1): 8.65 (s, 1H), 8.41 (J = 7.88, d, 1H), 8.28 (J = 8.44, d, 1H), 8.12 (s, 2H), 7.87 (J = 7.58, t, 1H), 7.77 (J = 7.76, t, 1H), 7.60 (J = 9.08, d, 1H), 6.90 (J = 11.12, d, 1H), 6.70 (s, 1H), 5.74 (s, 2H), 3.81 (J = 2.14, t, 1H), 3.58-3.53 (m, 4H), 1.17 (J = 6.98, t, 6H); ^{13}C NMR (100 MHz, DMSO-d_6), δ (ppm) (Figure S2): 172.1, 160.1, 157.7, 153.9, 145.3, 141.9, 132.4, 128.3, 124.8, 117.0, 111.5, 111.4, 109.4, 97.0, 50.5, 45.2, 22.5, 13.0, 11.5; HRMS (ESI) m/z: $[M]^+$ (Figure S3) calcd for: $C_{25}H_{23}N_2O_2S^+$, 415.1475; found, 415.1479.

CBTZ-acid: Compounds **3** and **2** were reacted by Knoevenagel to obtain the target product **CBTZ-acid**. **3** (0.90 g, 0.003 mol) and **2** (0.70 g, 0.003 mol) were refluxed with 0.2 mL of piperidine in 15.0 mL methanol for 4 h. After the reaction was complete, the solvent was evaporated. Then, the crude product was purified by silica gel column chromatography (CH_2Cl_2: CH_3OH = 10: 1, v/v), and black solid (0.74 g) was obtained with the yield of 47%. ^{1}H NMR (400 MHz, Methanol-d_4), δ (ppm) (Figure S4): 8.33 (s, 1H), 8.21 (J = 15.28, d, 1H), 8.14 (J = 7.92, d, 2H), 7.99 (J = 15.04, d, 1H), 7.79 (J = 7.46, t, 1H), 7.68 (J = 7.36, t, 1H), 7.51 (J = 8.92, d, 1H), 6.81 (J = 8.8, d, 1H), 6.53 (s, 1H), 5.00 (s, 2H), 3.53 (J = 7.84, d, 4H), 3.02 (s, 2H), 1.23 (J = 6.54, t, 6H); ^{13}C NMR (100 MHz, DMSO-d_6), δ (ppm) (Figure S5): 172.1, 160.1, 157.7, 153.9, 145.3, 141.9, 132.4, 128.3, 124.8, 117.0, 111.5, 111.4, 109.4, 97.0, 50.5, 45.2, 22.5, 13.0, 11.5; HRMS (ESI) m/z: $[M]^+$ (Figure S6): calcd for: $C_{25}H_{25}N_2O_4S^+$, 449.1530; found, 449.1529.

1.4 Detecting of Singlet Oxygen ($^1O_2$)

ABDA, a singlet oxygen capture agent, was used to measure the $^1O_2$ generated by **CBTZ-yne** or **CBTZ-acid**, respectively. Briefly, The absorbance peak of ABDA (0.049 μM) at 378 nm was recorded in aqueous solution. Then, 10 μM **CBTZ-yne** or **CBTZ-acid** was added and irradiated with light (LED lamp of 0.5 W/cm^2) for various time (0-80 s), and absorbance spectra of ABDA were measured immediately.

1.5 Detecting Reactive Oxygen Species (ROS)

DCFH-DA was used as the ROS indicator, which can be converted to 2', 7'-dichlorofluorescein (DCF) in the presence of ROS. **CBTZ-yne**, **CBTZ-acid**, and DCFH-DA were prepared as 10 μM in aqueous solution, respectively, which was exposed to light (LED lamp of 0.5 W/cm^2) for different time (0-35 s), and the fluorescence spectra with the excitation wavelength at 480 nm were observed immediately after each irradiation.

1.6 Detecting $O_2^{-\bullet}$ Generation *via* EPR Assay

The EPR assay was carried out with a Bruker Nano x-band spectrometer using 5, 5-dimethyl-1-pyrroline N-oxide (DMPO) as a spin-trap agent. **CBTZ-yne** and **CBTZ-acid** were dissolved in methanol at a dilution of 10^{-5} M, and then 25 mM DMPO was added into methanol without and with LED irradiation (0.5 W/cm^2 for 1 min) for 60 s. Finally, the EPR signals were recorded at room temperature.

1.7 Cell Culture and Imaging

Cells were cultured in cell culture dishes with Dulbecco's modified eagle medium (DMEM) medium containing 10% fetal bovine serum (FBS) and incubated at 37 °C in an air atmosphere (21% O_2). In fluorescence imaging experiments, the cells were planted into glass-bottom dishes (15 × 15 mm) at a density of 10^4 for confocal, co-location experiments and fluorescence lifetime imaging experiments.

1.8 Subcellular Co-localization Assay

HepG2 cells were plated onto 35 mm confocal dishes for 24 h. Next, the cells were firstly incubated with 10 μM **CBTZ-yne**, and **CBTZ-acid** for 30 min at 37 °C under 21% O_2 consideration, and stained by BODIPY, DAPI, respectively. Cells were then visualized with laser confocal microscopy. The excitation wavelength for **CBTZ-yne** and **CBTZ-acid** was 405 nm and 561 nm, BODIPY was 488 nm, and DAPI was 405 nm. The emission wavelength of **CBTZ-acid** was collected from 480 to 510 nm and 650-680 nm, 480-510 nm and 650-680nm for **CBTZ-yne**, 510-540 nm for BODIPY, 500-530 nm for DAPI.

1.9 Detecting Intracellular ROS

DCFH-DA was applied for intracellular ROS detection. The HepG2 cells were incubated with 10 μM **CBTZ-yne** and **CBTZ-acid** for 30 min for cell uptake followed by incubation with 10 μM DCFH-DA for 30 min, respectively. After that, the cells were washed with PBS three

times and irradiated for different times. The green fluorescence was immediately observed using CLSM. (λ_{ex} = 488 nm; λ_{em} = 530 nm).

1.10 γ-H2AX Immunofluorescence Staining Assay

HepG2 cells were plated onto 35 mm confocal dishes for 24 h. Next, the cells were firstly incubated with 10 μM **CBTZ-yne**, and **CBTZ-acid** for 30 min at 37 °C under 21% O_2 consideration, respectively, then treated with γ-H2AX rabbit monoclonal antibody and anti-rabbit 488 (according to instructions), and finally stained with DAPI for 5 min. Cells were then visualized with laser confocal microscopy. The excitation wavelength for DAPI and γ-H2AX was 405 nm and 495 nm. The emission wavelength of DAPI and γ-H2AX was 430 nm and 520 nm.

1.11 In Vitro Cytotoxicity Assay

HepG2 cells were plated at 10^4 cells per well in a 96 well cell culture plate, followed by incubation at 37 °C for 24 h. **CBTZ-yne** and **CBTZ-acid** with varying concentrations were added into each well, and cultured for another 30 min in dark. After that, the cell culture media was replaced with 200 μL fresh medium. Then, 20 μL MTT solutions (5 mg/mL) in PBS were added to each well. After incubating the cells for 4 h, the medium was removed out carefully, and 200 μL DMSO was added to each well to dissolve blue formazan. Finally, the absorbance of 490 nm was measured with a Bio-Rad microplate reader and the cell viability was calculated by the following equation: cell viability (%) = (mean of abs. value of treatment group/mean abs . value of control)×100%.

Then photo induced cell viability was employed for treatment, after irradiation 30 min, cells were allowed to continue growing for 24 h and all other steps were the same as above.

1.12 Docking

CBTZ-yne and **CBTZ-acid** small molecule structures were hydrogenated and minimized with energy. The DNA (PDB: 5JU4) was minimized with energy. The active site of DNA molecules was set to allow small molecules to be docked into in any conformation and position. **CBTZ-yne** and **CBTZ-acid** was used as ligands and DNA as receptor for molecular docking CDOCKER operation.

2. Supporting Scheme

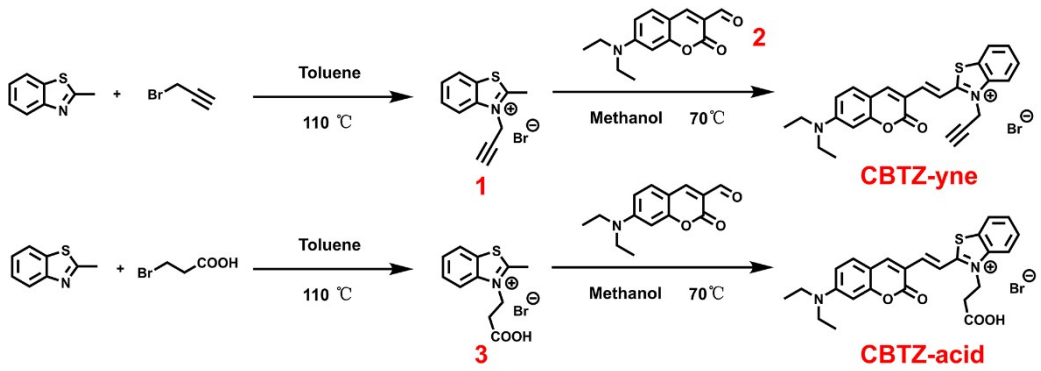

Scheme S1. Synthetic route to compounds of **CBTZ-yne** and **CBTZ-acid**.

3. Supporting Figures

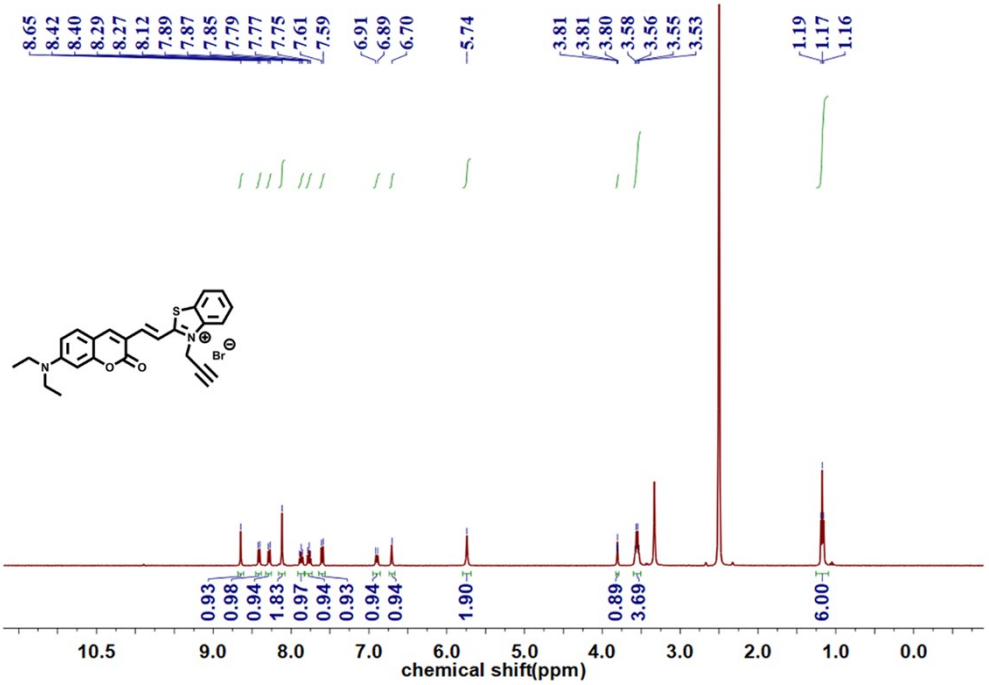

Figure S1. ^{1}H-NMR spectrum of **CBTZ-yne** in DMSO-d_6.

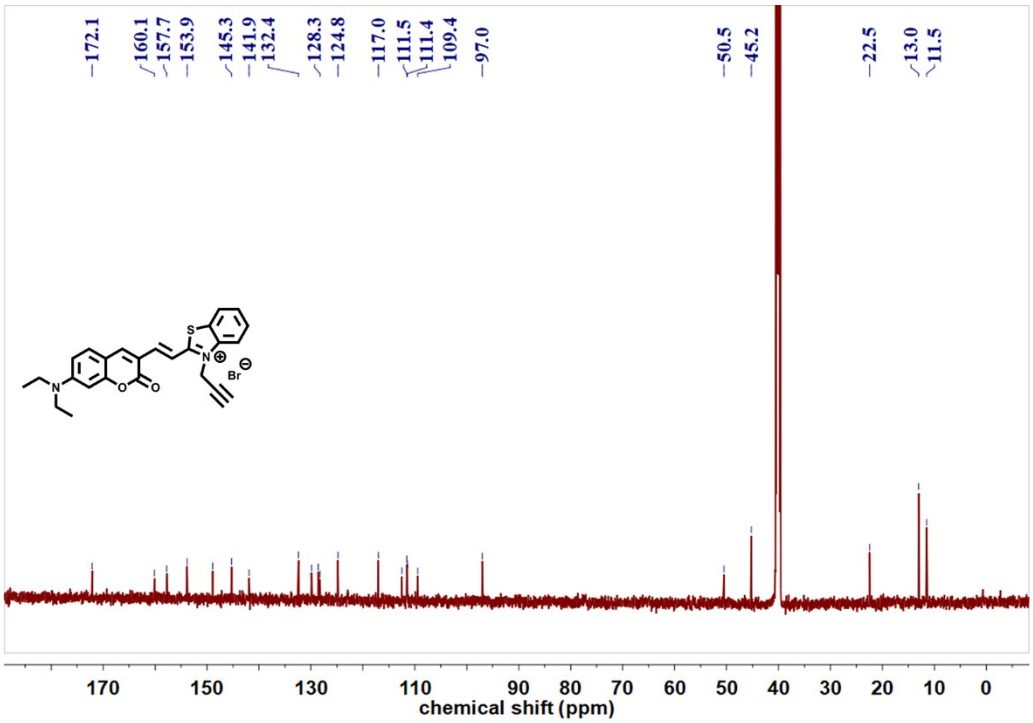

Figure S2. ^{13}C-NMR spectrum of **CBTZ-yne** in DMSO-d_6.

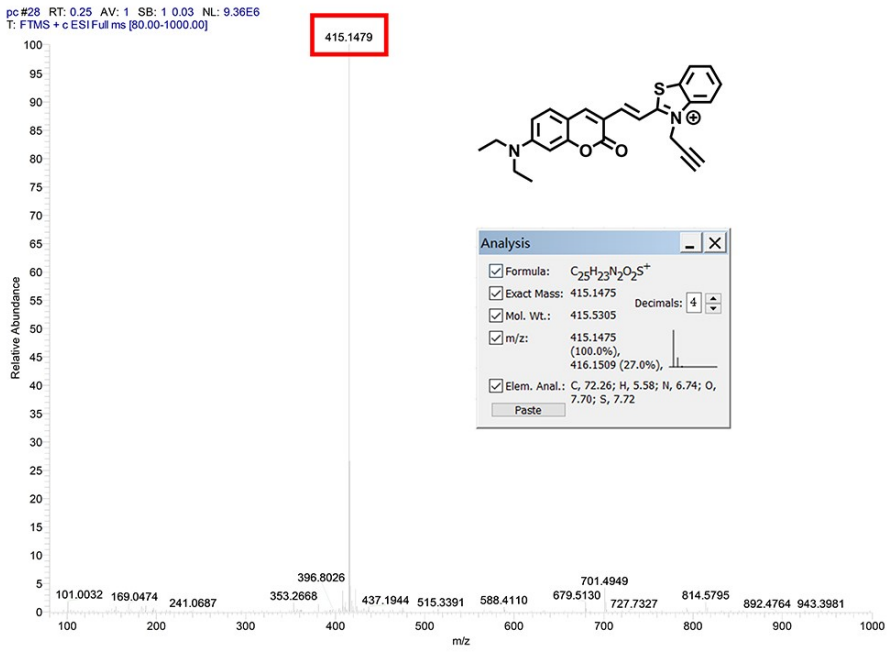

Figure S3. HRMS of **CBTZ-yne** in methanol.

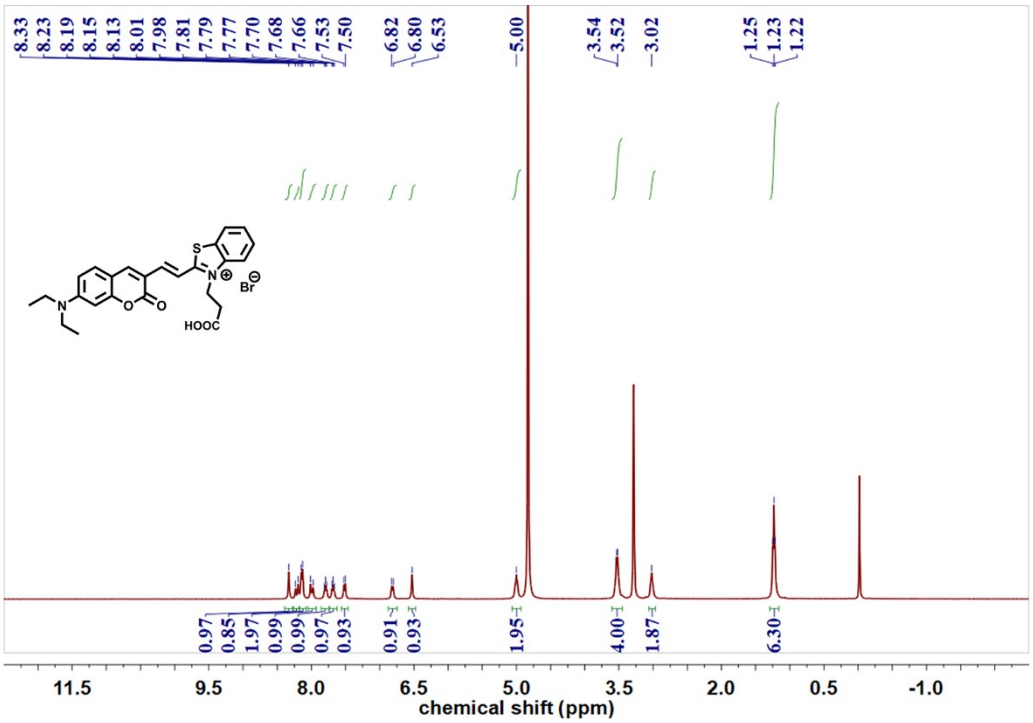

Figure S4. ^{1}H-NMR spectrum of **CBTZ-acid** in DMSO-d_6.

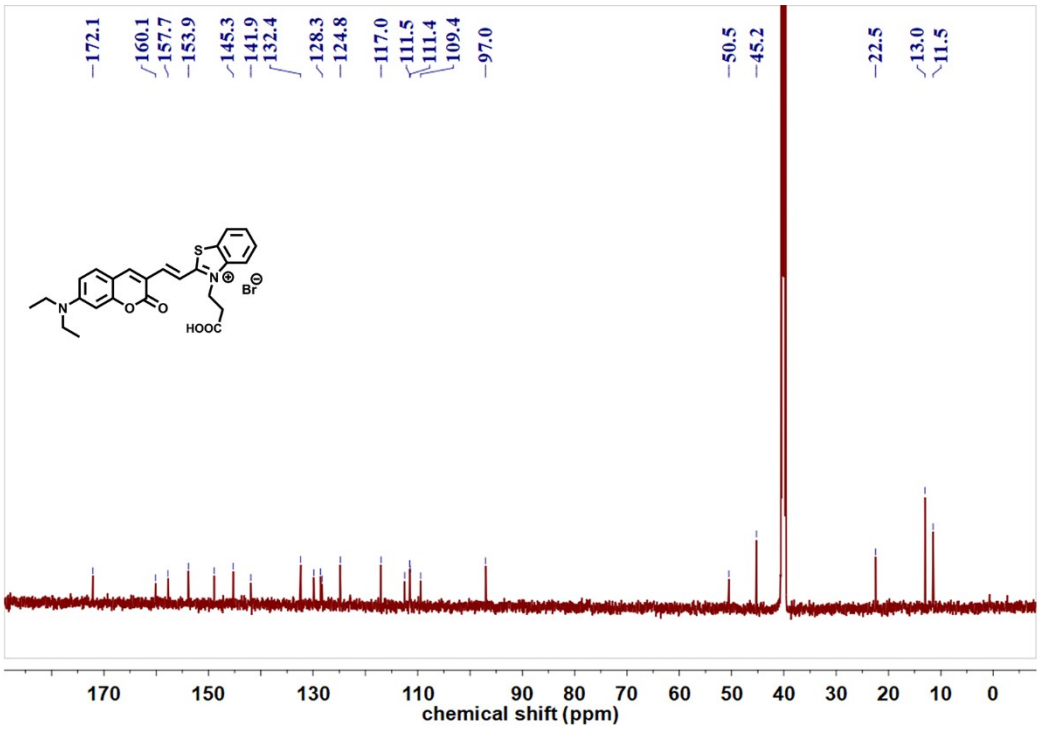

Figure S5. ^{13}C-NMR spectrum of **CBTZ-acid** in DMSO-d_6.

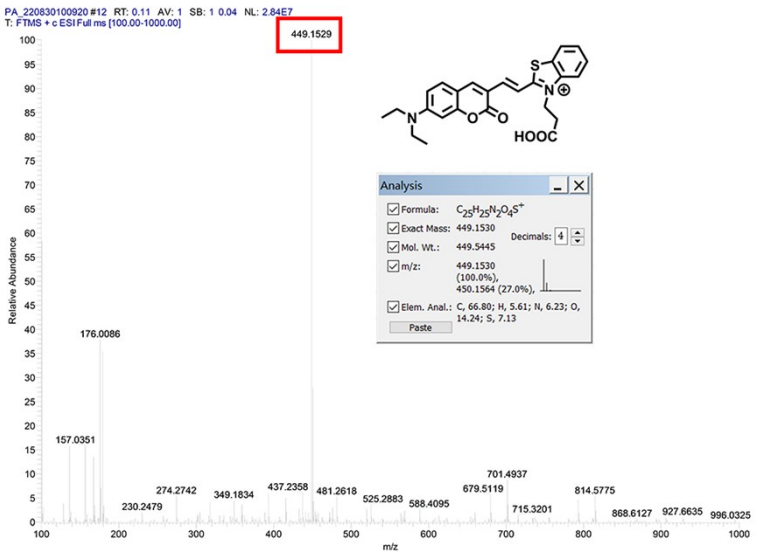

Figure S6. HRMS of **CBTZ-acid** in methanol.

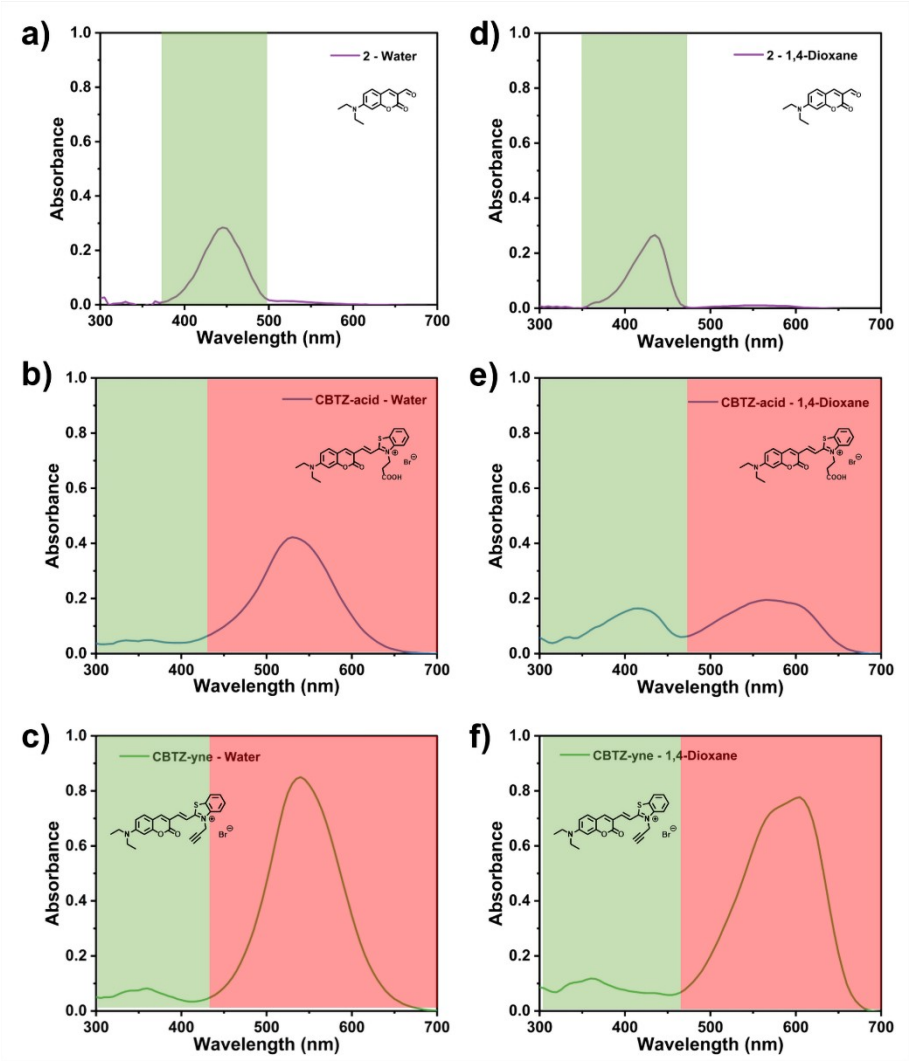

Figure S7. The absorbance spectra of **2, CBTZ-acid,** and **CBTZ-yne**, respectively.

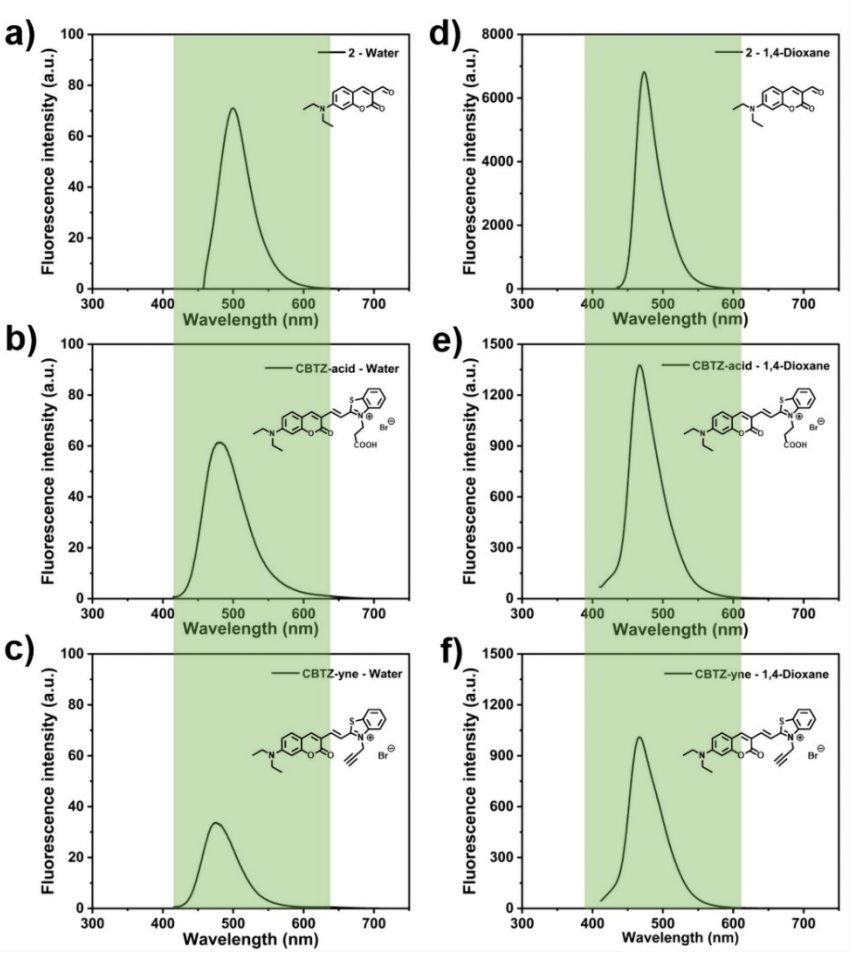

Figure S8. The fluorescence spectra of **2, CBTZ-acid,** and **CBTZ-yne**, respectively (λ_{ex} = 405 nm).

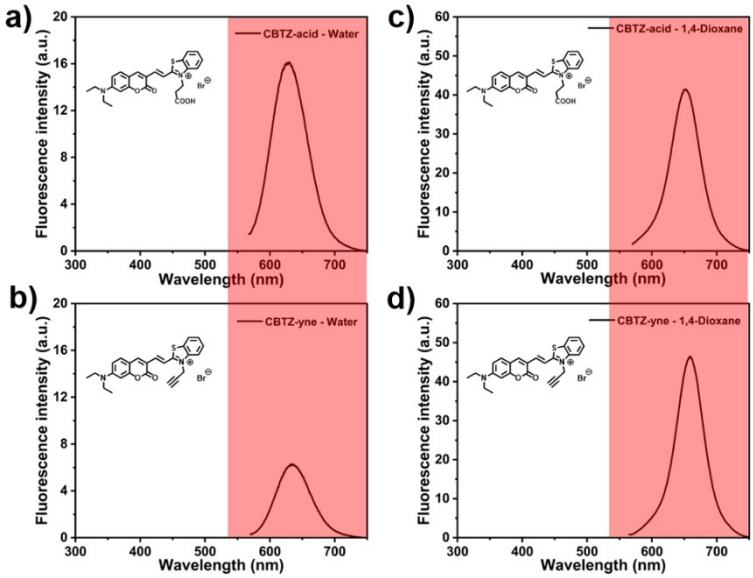

Figure S9. The fluorescence spectra of **CBTZ-acid**, and **CBTZ-yne**, respectively (λ_{ex} = 561 nm).

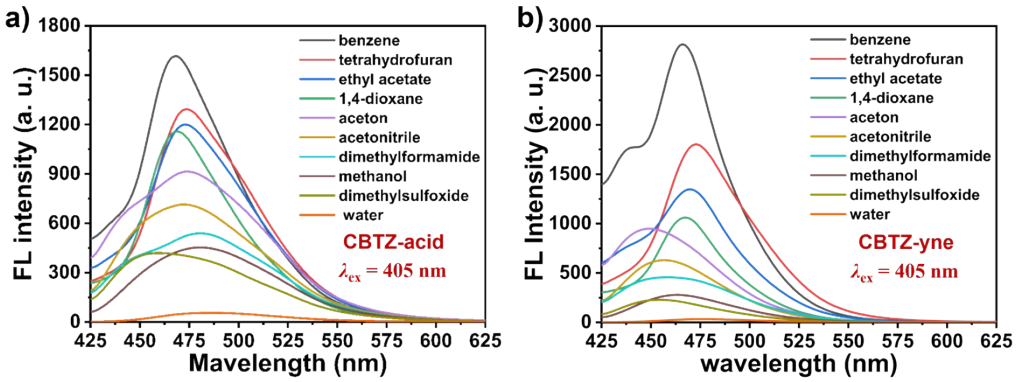

Figure S10. The fluorescence spectra of a) **CBTZ-acid** and b) **CBTZ-yne** in different solvents, respectively. (λ_{ex} = 405 nm).

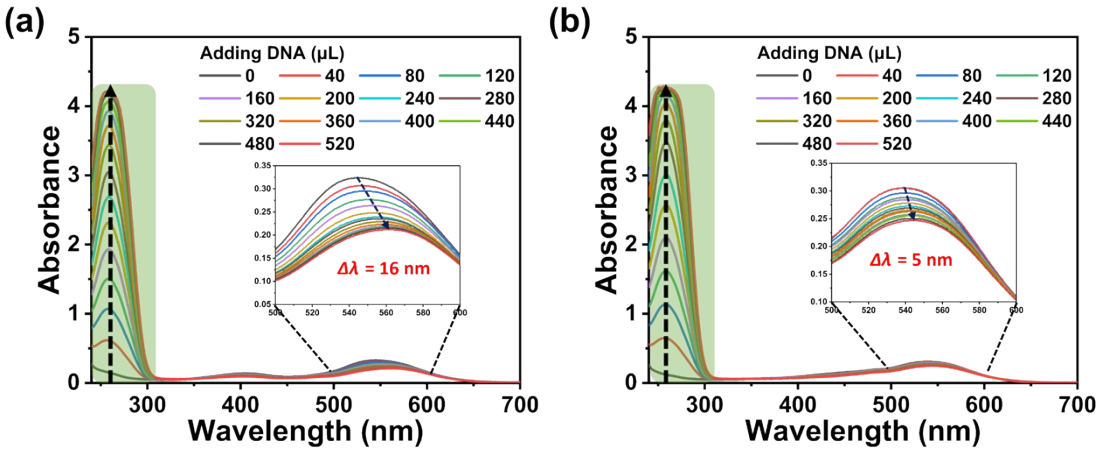

Figure S11. a) Absorbance spectra of **CBTZ-yne** (10^{-5} M) in Tris-HCl buffer (pH 7.4) with increasing concentrations of DNA (0 - 520 μL, 2 mg/mL). b) Absorbance spectra of **CBTZ-acid** (10^{-5} M) in Tris-HCl buffer (pH 7.4) with increasing concentrations of DNA (0 - 520 μL, 2 mg/mL).

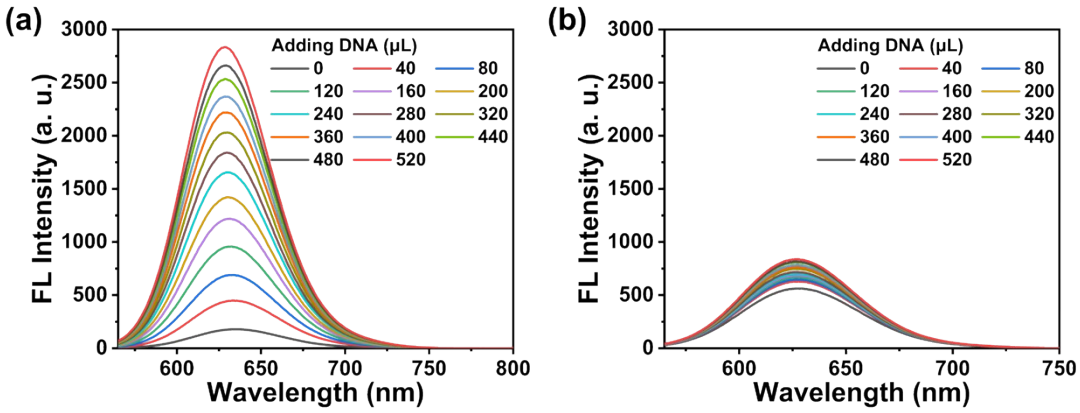

Figure S12. Fluorescence spectra of **CBTZ-yne** (10 μM) a) and **CBTZ-acid** (10 μM) b) in Tris-HCl buffer with increasing concentrations of DNA (0 - 520 μL, 2 mg/mL), respectively.

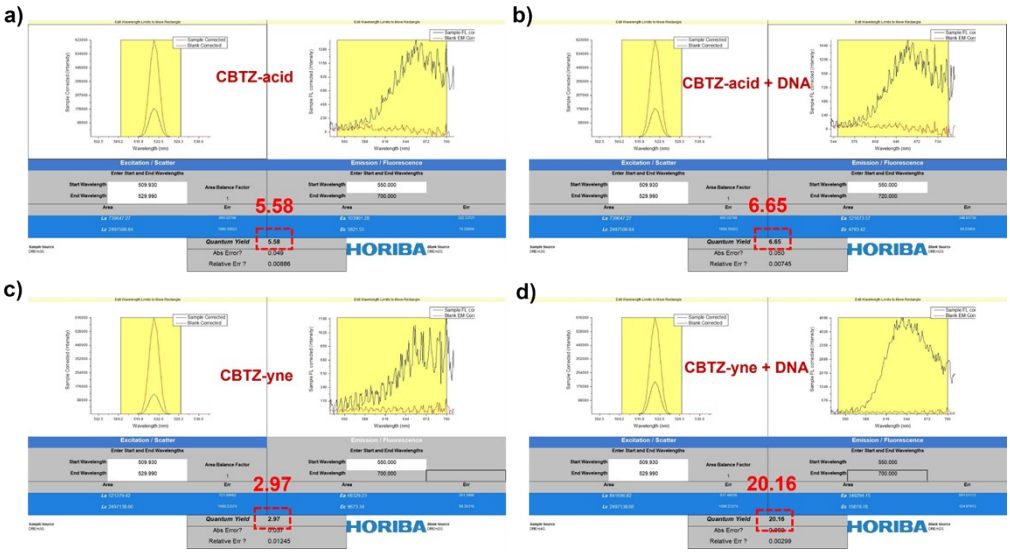

Figure S13. The fluorescence quantum yield of a) **CBTZ-acid** (10^{-5} M), b) **CBTZ-acid** + DNA (520 μL), c) **CBTZ-yne** (10^{-5} M), d), **CBTZ-yne** (10^{-5} M) + DNA (520 μL) in aqueous solution.

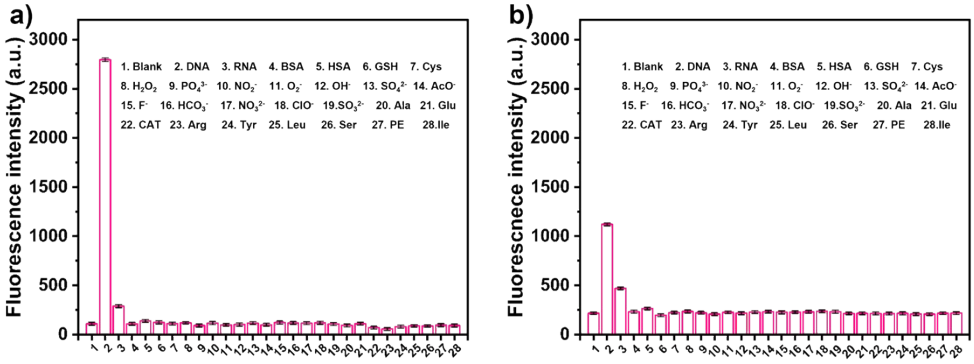

Figure S14. The selectivity of a) **CBTZ-yne** and b) **CBTZ-acid** responses to various analytes (concentration, 60 μM).

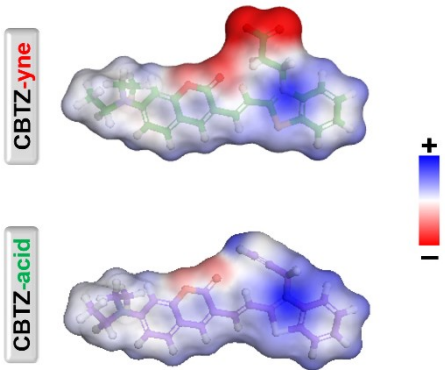

Figure S15. Electrostatic potential (ESP) profiles of **CBTZ-yne** and **CBTZ-acid**.

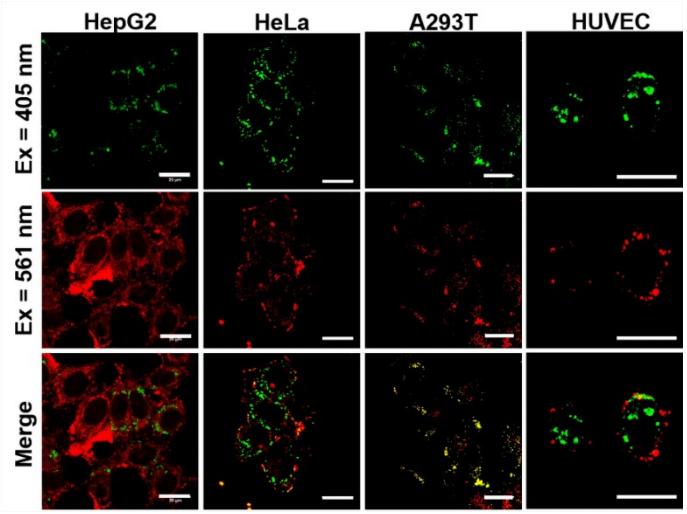

Figure S16. HepG2, HeLa, A293T, and HUVEC cells incubated by **CBTZ-acid** for confocal microscopic imaging, respectively. Scale bar: 20 μM.

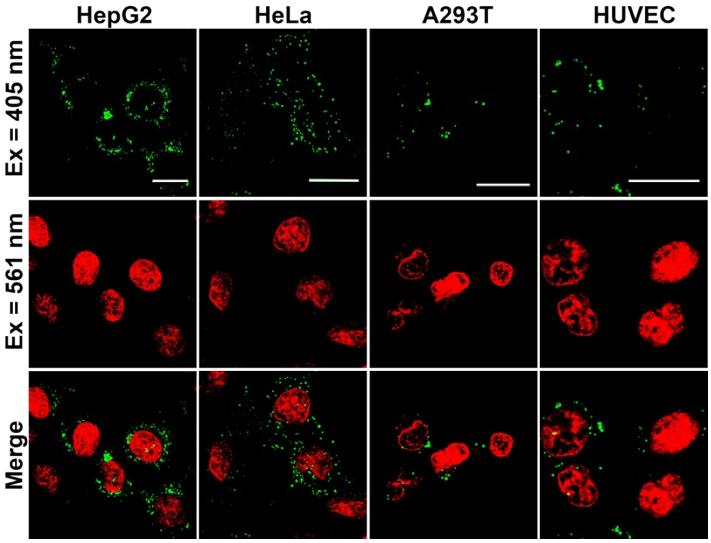

Figure S17. HepG2, HeLa, A293T, and HUVEC cells incubated by **CBTZ-yne** for confocal microscopic imaging, respectively. Scale bar: 20 μM.

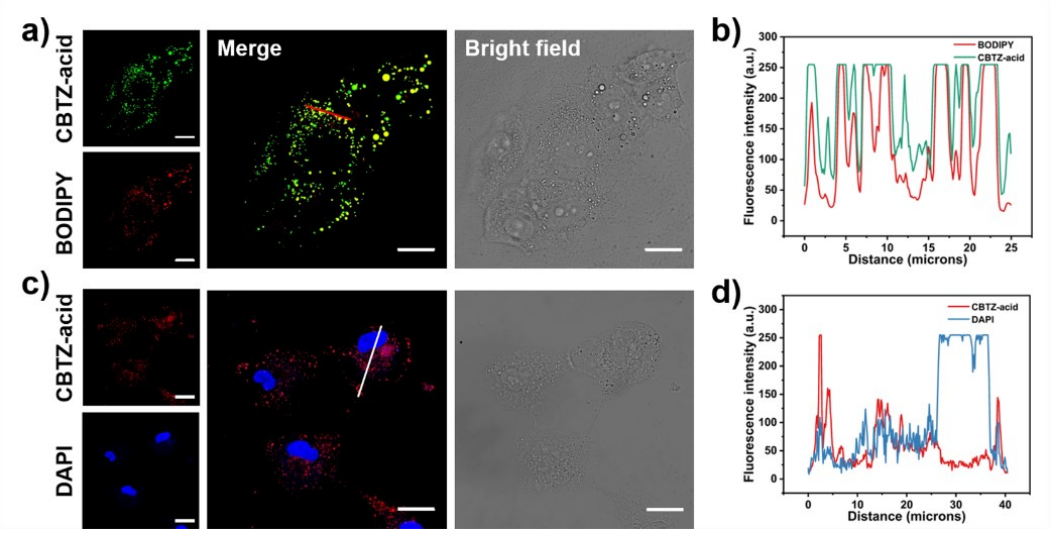

Figure S18. a) Co-localization analysis of the HepG2 cells incubated by **CBTZ-acid** and co-stained with BODIPY, b) The curve of fluorescence intensity at the red line of **CBTZ-acid** and BODIPY colocalization images of a). c) Co-localization analysis of the HepG2 cells incubated by **CBTZ-acid** and co-stained with DAPI, d) Fluorescence intensity curve at the white line of **CBTZ-acid** and DAPI colocalization images of c). Scale bar: 20 μM.

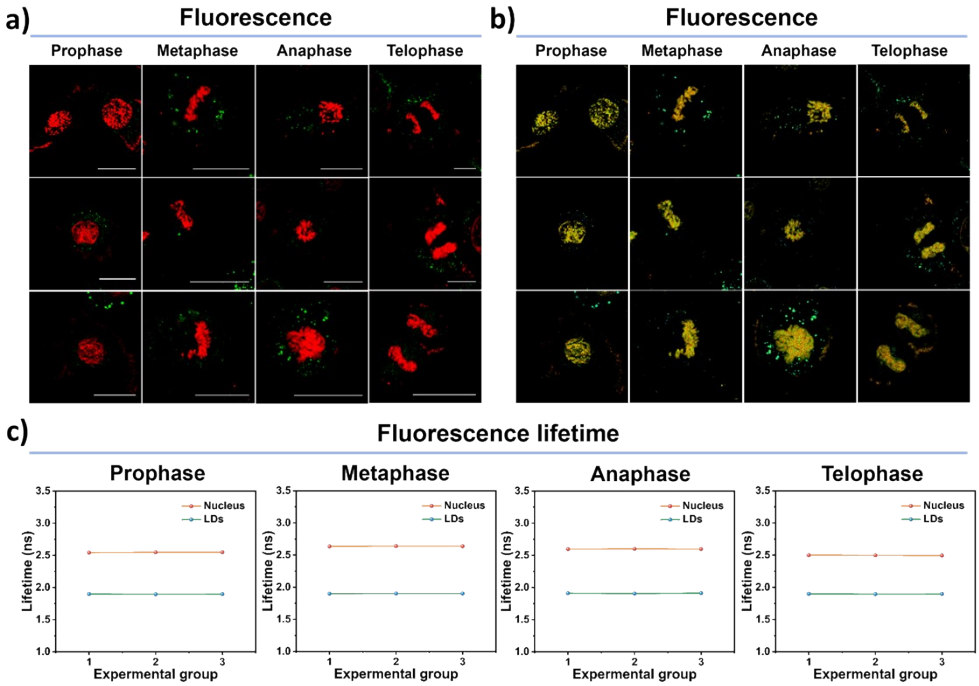

Figure S19. The confocal fluorescence images for lipid droplets and nucleus in HepG2 cells incubated in **CBTZ-yne** (10 μM) at different mitosis periods; b) The fluorescence lifetime imaging for lipid droplets and nucleus in HepG2 cells incubated in **CBTZ-yne** (10 μM); c) The fitted average fluorescence lifetime curves of Nucleus and LDs in HepG2 cells of (b). Scale bar: 20 μM, (n=3).

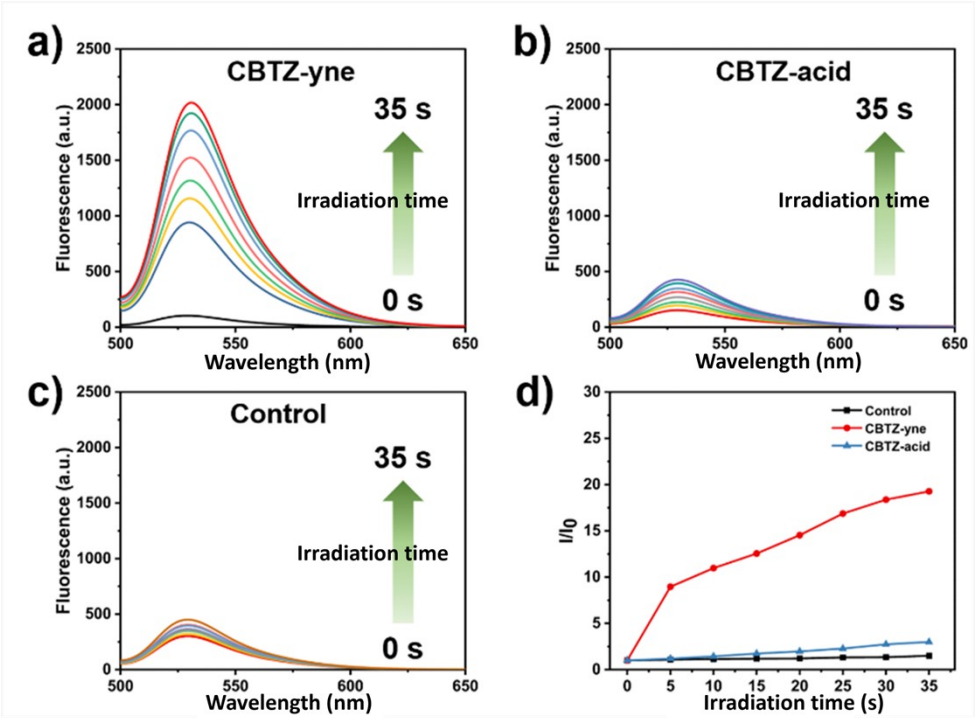

Figure S20. The detection of ROS generated upon irradiation of LED lamp using DCFH-DA, a) **CBTZ-yne**, b) **CBTZ-acid**, and c) **Control** groups, respectively; d) Plotting of fluorescent intensity of DCF (λ_{em} = 525 nm) with different irradiation time (0-35 s) upon LED lamp (0.5 W/cm^2).

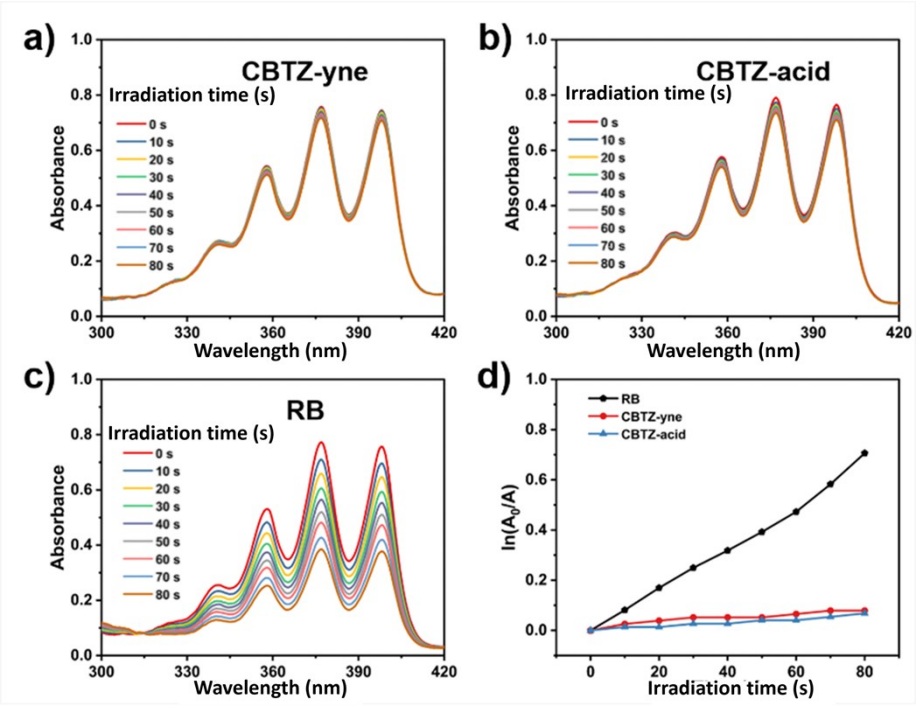

Figure S21. The detection of $^1O_2$ generated upon irradiation of LED lamp using ABDA, a) **CBTZ-yne**, b) **CBTZ-acid**, and c) **RB** groups, respectively; d) Plotting of the absorbance of ABDA (λ_{ex} = 378 nm) with different irradiation time (0-80 s) upon LED lamp (0.5 W/cm^2).

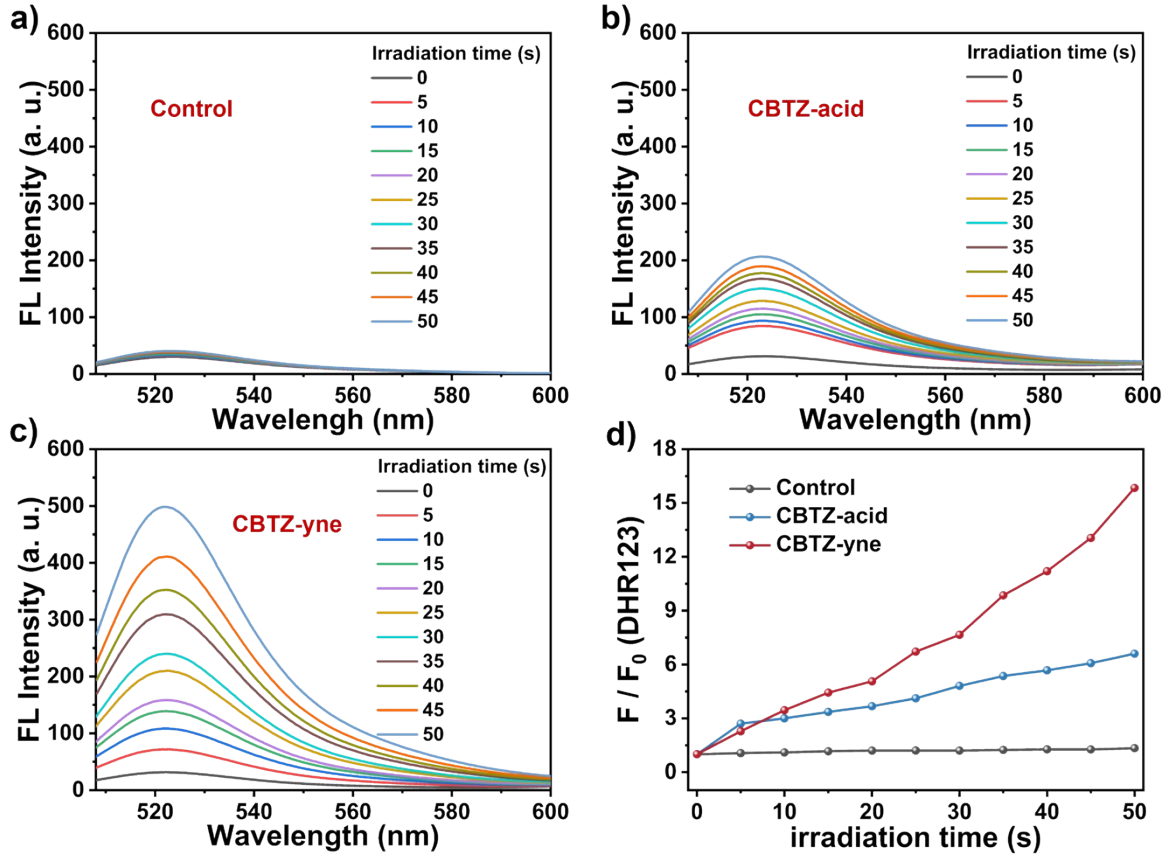

Figure S22. The detection of $O_2^{-\bullet}$ generated by **CBTZ-acid** and **CBTZ-yne** with different irradiation time (0-50 s) upon irradiation of LED lamp (0.5 W/cm^2) using DHR123 as a fluorescent indicator.

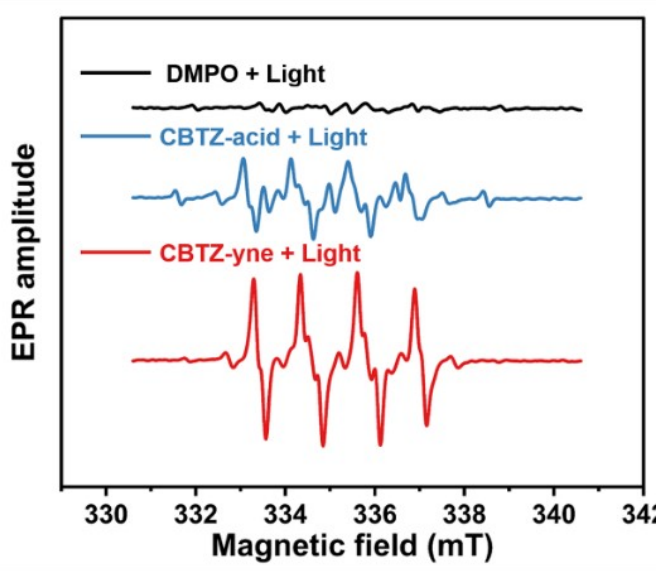

Figure S23. EPR spectra of **CBTZ-acid**, and **CBTZ-yne** with the presence of DMPO irradiated by LED lamp.

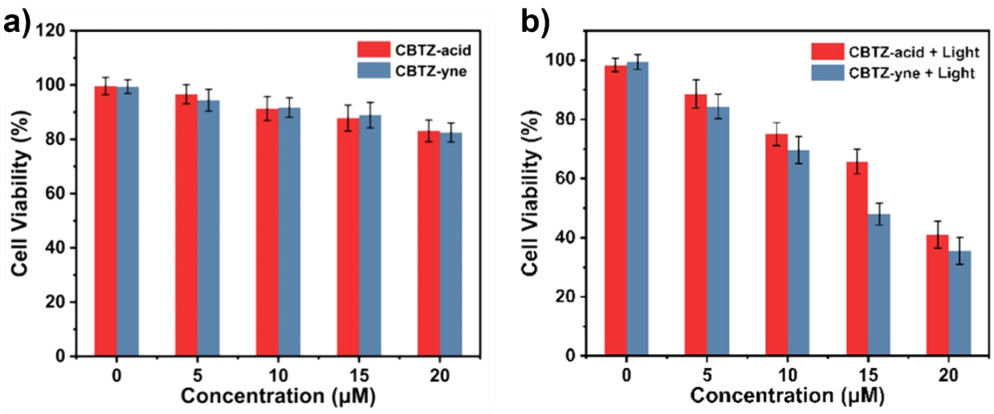

Figure S24. The viabilities of HepG2 cells incubated with **CBTZ-yne** or **CBTZ-acid** a) in dark, b) under the irradiation of LED lamp (0.5 W/cm^2) for 10 min.

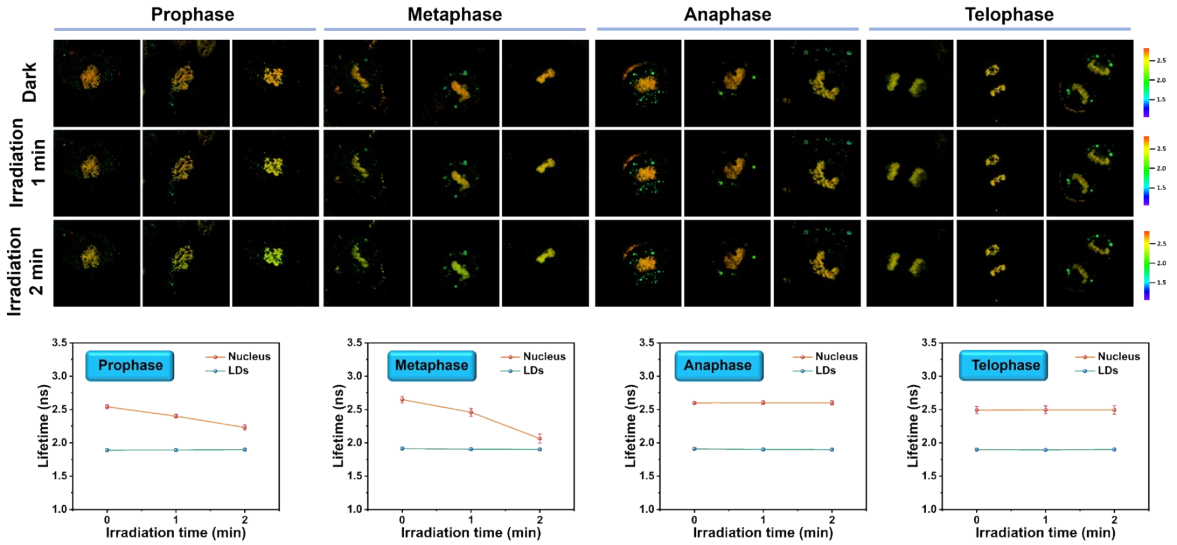

Figure S25. The fluorescence lifetime of **CBTZ-yne** in lipid droplets and nucleus in HepG2 cells during mitosis under the influence of ROS by FLIM; Quantitative plot of fluorescence lifetime.

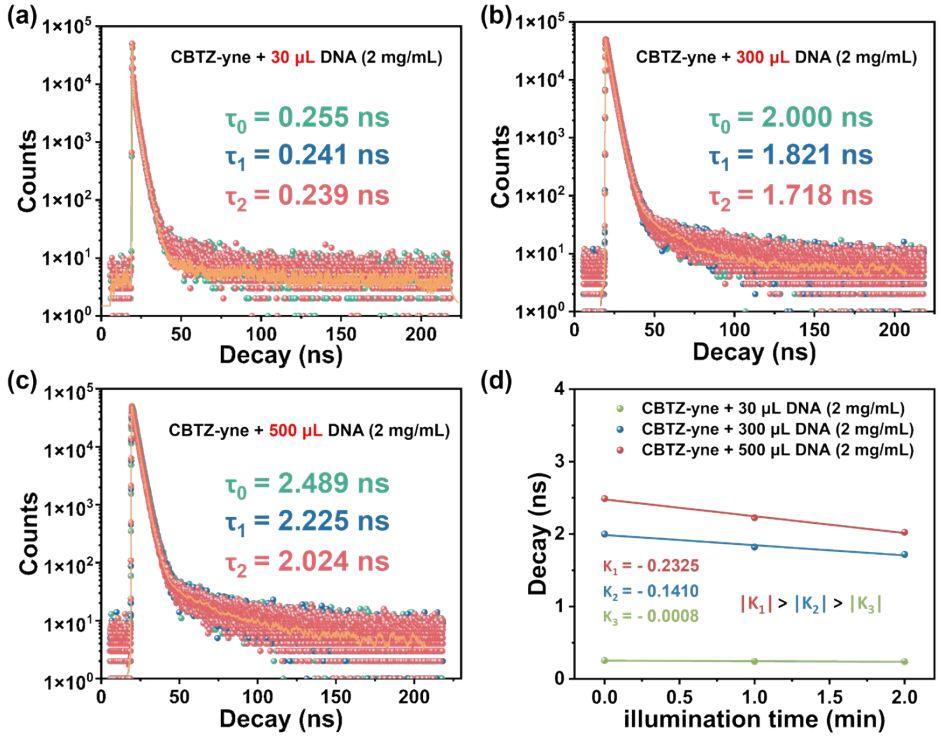

Figure S26. The fluorescence lifetime of **CBTZ-yne** (Tris-HCl buffer, 10-5 M) + a) 30 μL, b) 300 μL, c) 500 μL DNA (aqueous solution, 2 mg/mL) under different light times. d) Fitting linear relationship of fluorescence lifetime, *K*: slope.

4. Supporting Table

Table S1. The data of Docking calculation about **CBTZ-acid** binding DNA.

Name	Stage	Forcefield	Start Time (ps)	End Time (ps)	Initial Potential Energy (kcal/mol)	Total Energy (kcal/mol)	Potential Energy (kcal/mol)	Kinetic Energy (kcal/mol)	Temperature (K)	Vander Waals Energy (kcal/mol)	Electrostatic Energy (kcal/mol)	Initial RMS Gradient (kcal/(mol x A))	Final RMS Gradient (kcal/(mol x A))
CBTZ-acid	Minimization	5JU4-CHARMm			-30927.159		-31000.692			2792.947	-22530.944	0.522	0.100
CBTZ-acid	Minimization2	5JU4-CHARMm			-31000.692		-31748.833			2679.306	-22896.573	0.100	0.220
CBTZ-acid	Heating	5JU4-CHARMm	0.000	4.000	-31748.833	-22258.319	-26491.018	4232.699	287.701	1629.010	-17436.661	17.102	17.186
CBTZ-acid	Equilibration	5JU4-CHARMm	4.000	104.000	-26491.018	-22461.762	-26834.415	4372.652	297.213	1479.705	-17388.734	17.186	17.335
CBTZ-acid	Production	5JU4-CHARMm	104.000	204.000	-26834.415	-22533.125	-26953.576	4420.451	300.462	1549.621	-17480.845	17.335	17.336

5. References

1. L. Unger-Angel, B. Rout, T. Ilani, M. Eisenstein, L. Motiei, D. Margulies, *Chemical Science* **2015**, *6*, 5419-5425.
2. J.-S. Wu, W.-M. Liu, X.-Q. Zhuang, F. Wang, P.-F. Wang, S.-L. Tao, X.-H. Zhang, S.-K. Wu, S.-T. Lee, *Organic Letters* **2007**, *9*, 33-36.
3. Y. Zhao, C. Zhang, J. Liu, D. Li, X. Tian, A. Wang, S. Li, J. Wu, Y. Tian, *Journal of Materials Chemistry B* **2019**, *7*, 3633-3638.